Electronic Supplementary Material (ESI) for Journal of Materials Chemistry A.

Electronic Supplementary Information

High Conductivity Enabled by Concerted Li Ion Diffusion in $Li_3Y(Br_3Cl_3)$ Solid Electrolytes for All-Solid-State Batteries

Taegon Jeon and Sung Chul Jung*

Department of Physics, Pukyong National University, Busan, 48513, Republic of Korea

Corresponding Author

*E-mail: scjung@pknu.ac.kr

(a) TM layer – Y atoms (b) TM layer – Li atoms

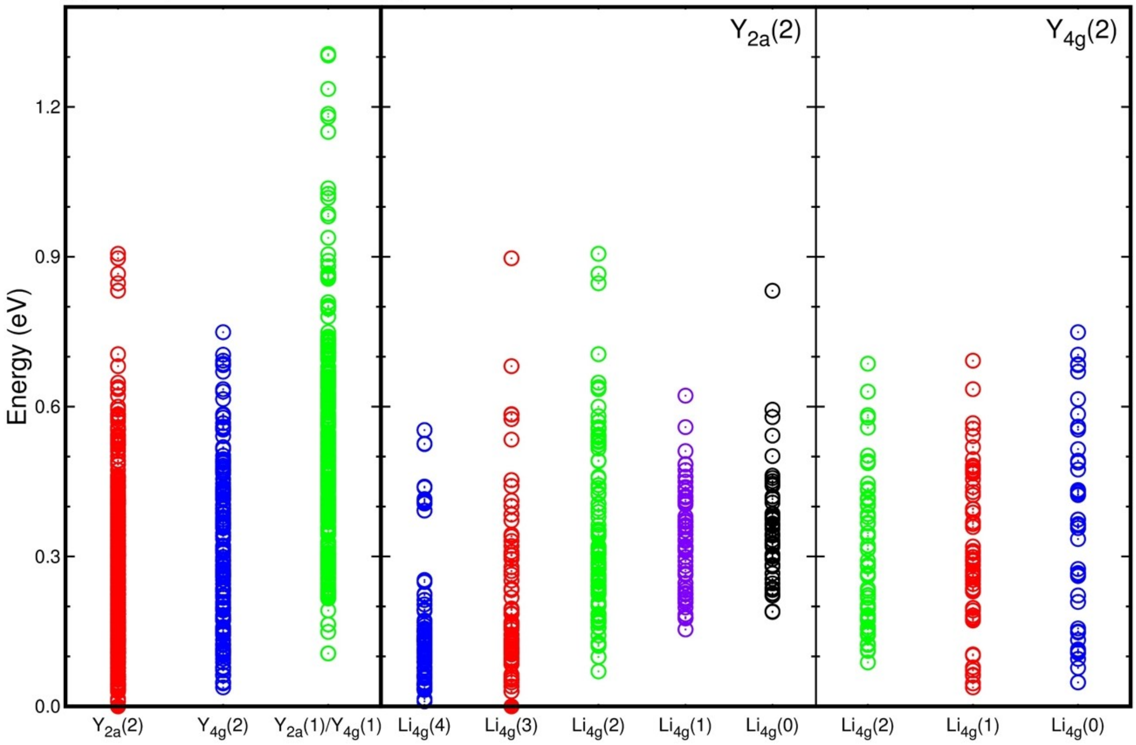

(c) Li layer – Li atoms

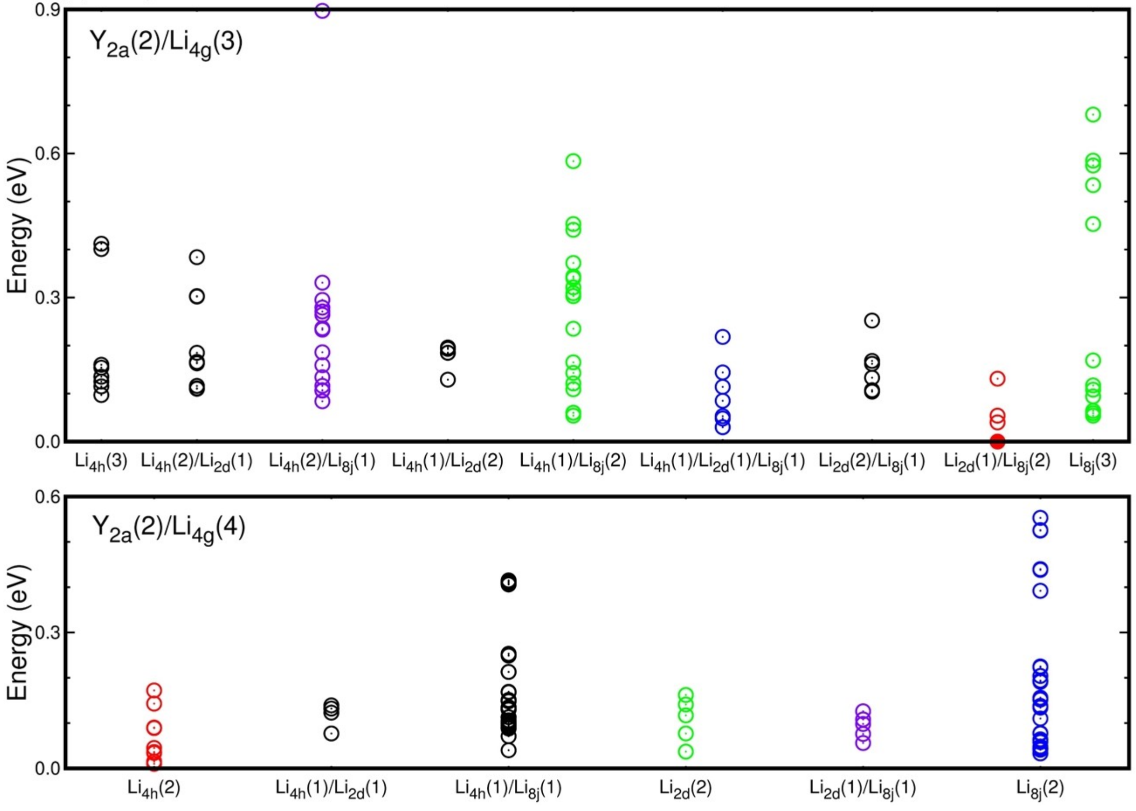

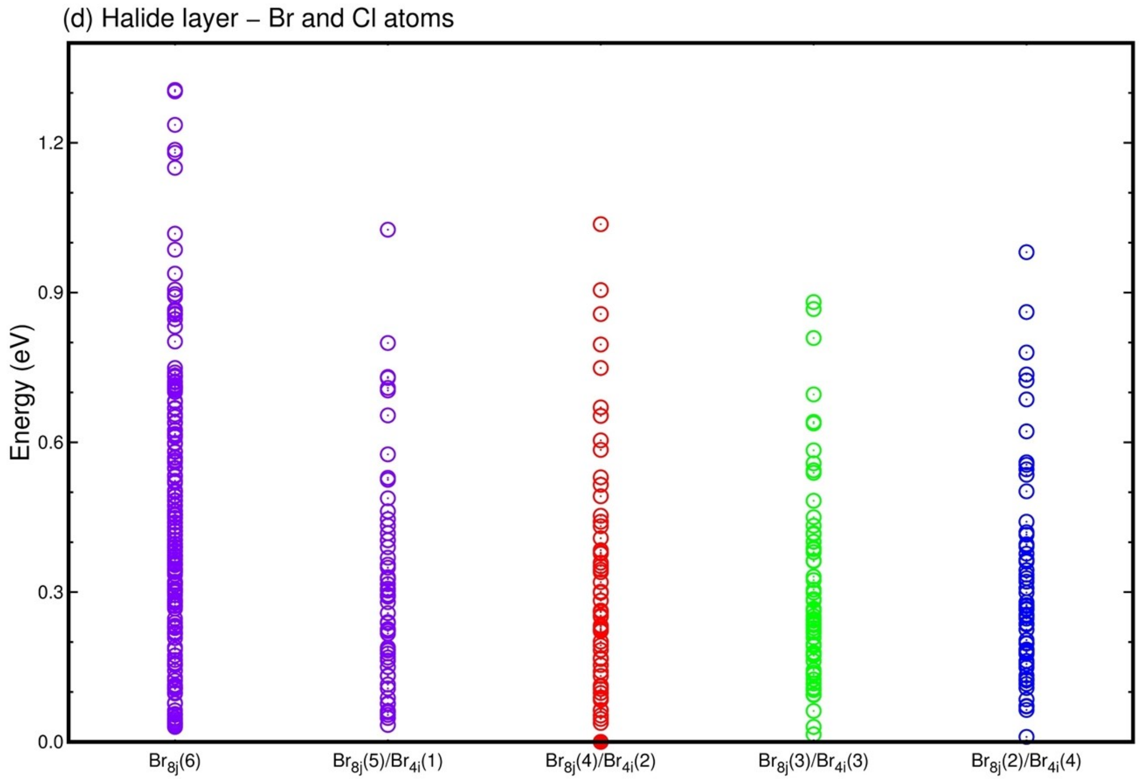

Fig. S1 Relative energies of all the investigated $Li_3Y(Br_3Cl_3)$ (LYBC) structures sorted by different configurations of (a) Y atoms in the Y layer, (b) Li atoms in the Y layer, (c) Li atoms in the Li layer, and (d) Br and Cl atoms in the halide layer. $X_A(n)$ represents n X atoms occupying the A site.

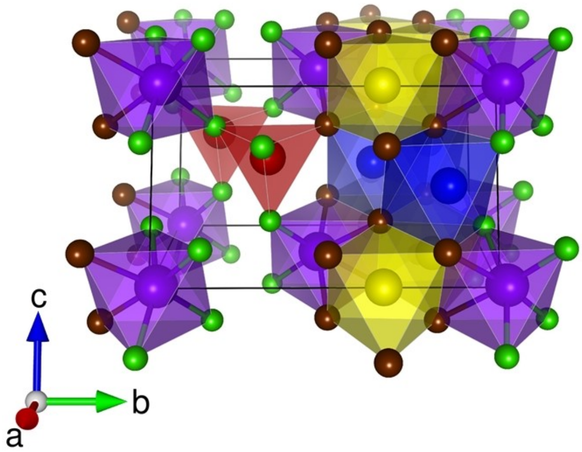

Fig. S2 Polyhedral representation of model B, in which the 4h (O_h) sites in the Li layer are occupied.

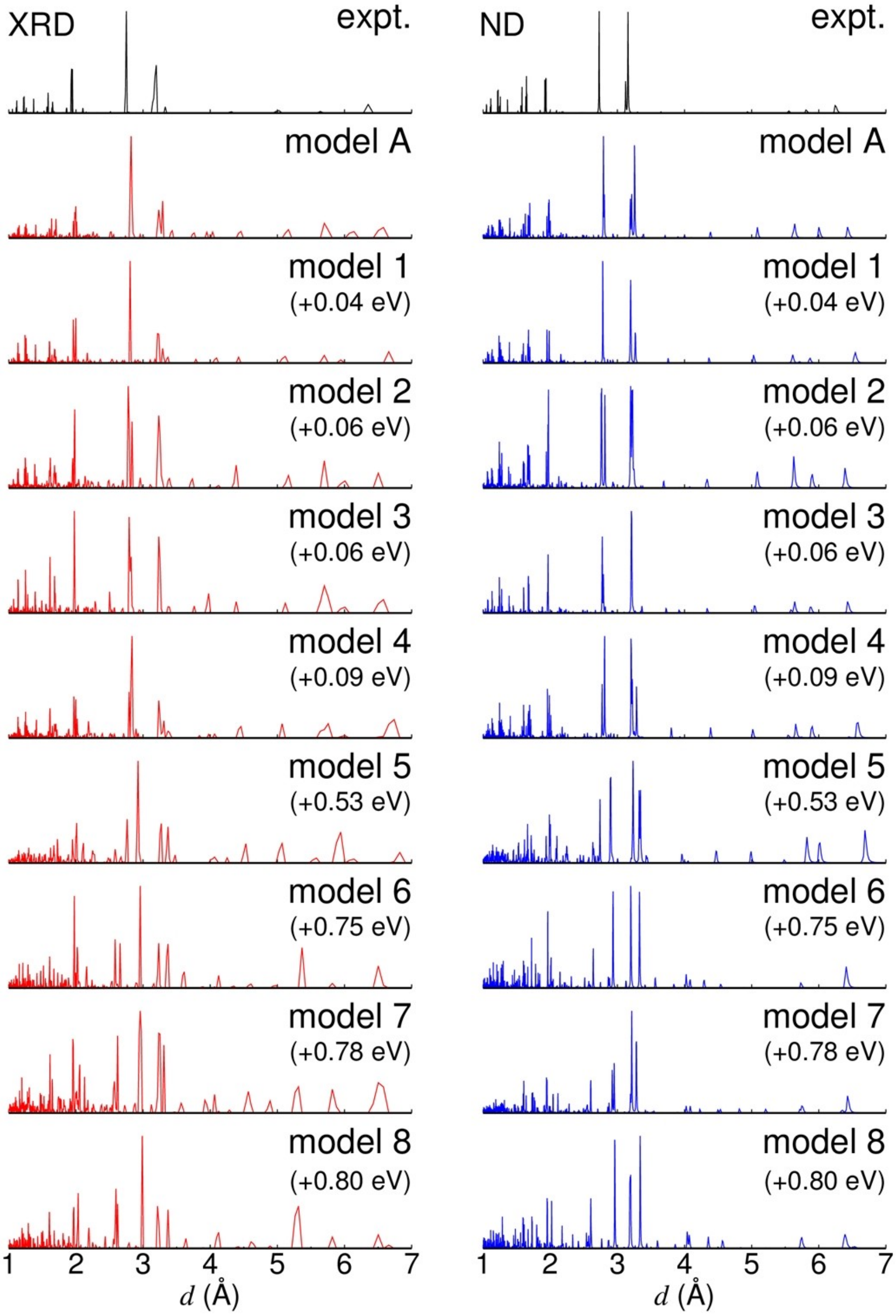

Fig. S3 Simulated synchrotron X-ray diffraction (XRD) and neutron diffraction (ND) patterns of model A and metastable LYBC structures (models 1–8). Numbers in parentheses represent relative energies per the 1 × 1 × 1 unit cell with respect to model A. The experimental patterns were obtained by simulating the diffraction patterns of the structural model shown in Fig. 1a.

LYBC models with stacking faults

We simply simulated four LYBC models with stacking faults using the 1 × 1 × 5 unit cell containing 30 Li, 10 Y, 30 Br, and 30 Cl atoms (Fig. S4†). In our stacking fault models, two of the five Y layers in the unit cell are displaced from the (0, 0, *h*) positions to the (1/2, 1/6, *h*) positions, resulting in a site change from 2a to 4g of all Y atoms in the fourth and fifth layers. This movement of Y atoms greatly reduces the occupancy of Y atoms at the 2a site at Y–Y distances larger than about 20 Å in the *c*-axis direction and changes the average configuration of all Y atoms in the unit cell from $Y_{2a}(2)$ to $Y_{2a}(1.22)/Y_{4g}(0.78)$ (Table S1†), which are in good agreement with the experimental reports.[1] In models S1 and S2, only Y atoms are displaced, but in models S3 and S4, Br and Cl atoms are also displaced in the same way as Y atoms. There is a difference in the arrangement of Li ions between models S1 and S2, and the same is true between models S3 and S4.

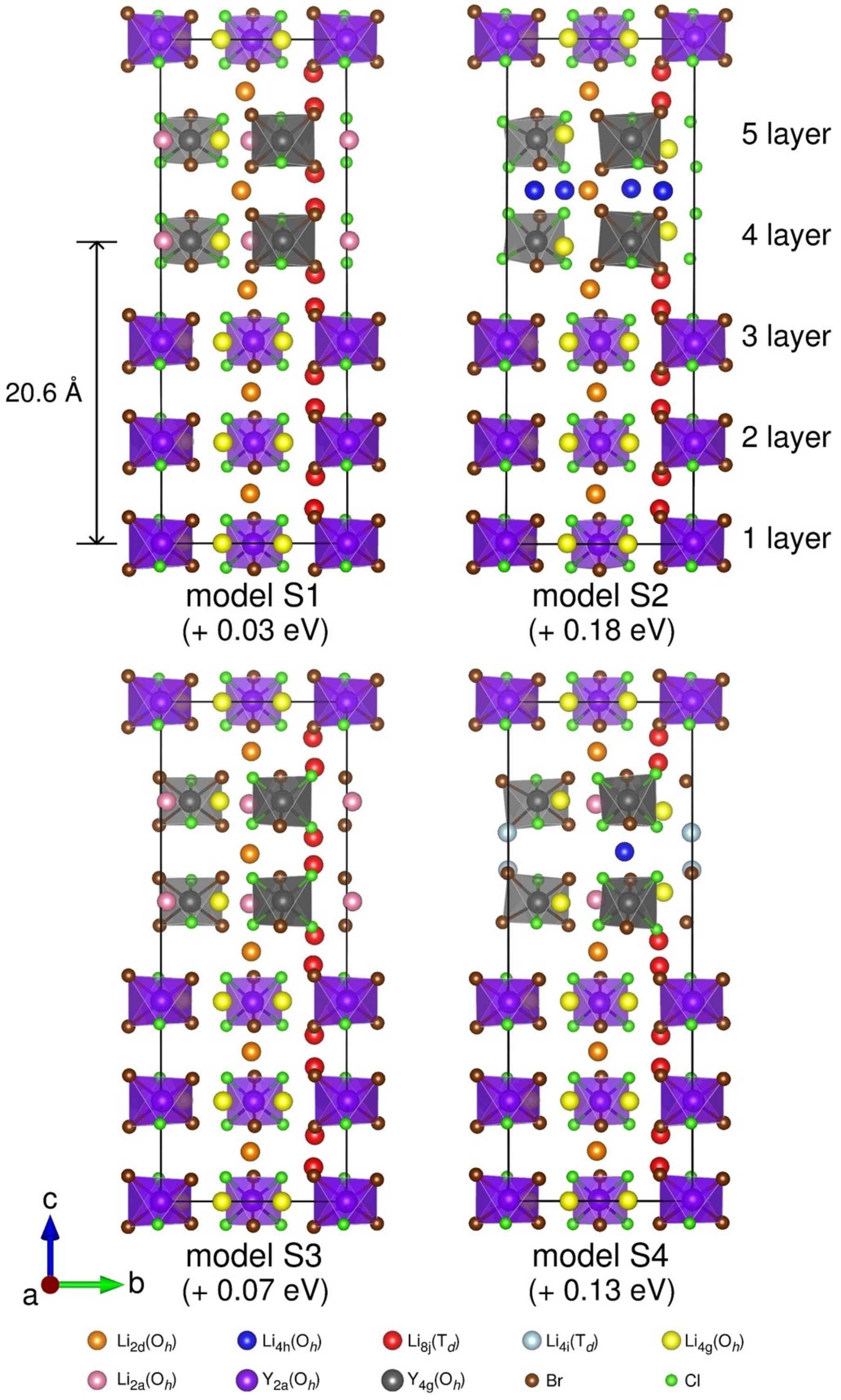

Fig. S4 LYBC models with stacking faults (models S1–S4). Solid lines represent the 1 × 1 × 5 unit cell. Numbers in parentheses represent relative energies per the 1 × 1 × 1 unit cell with respect to model A.

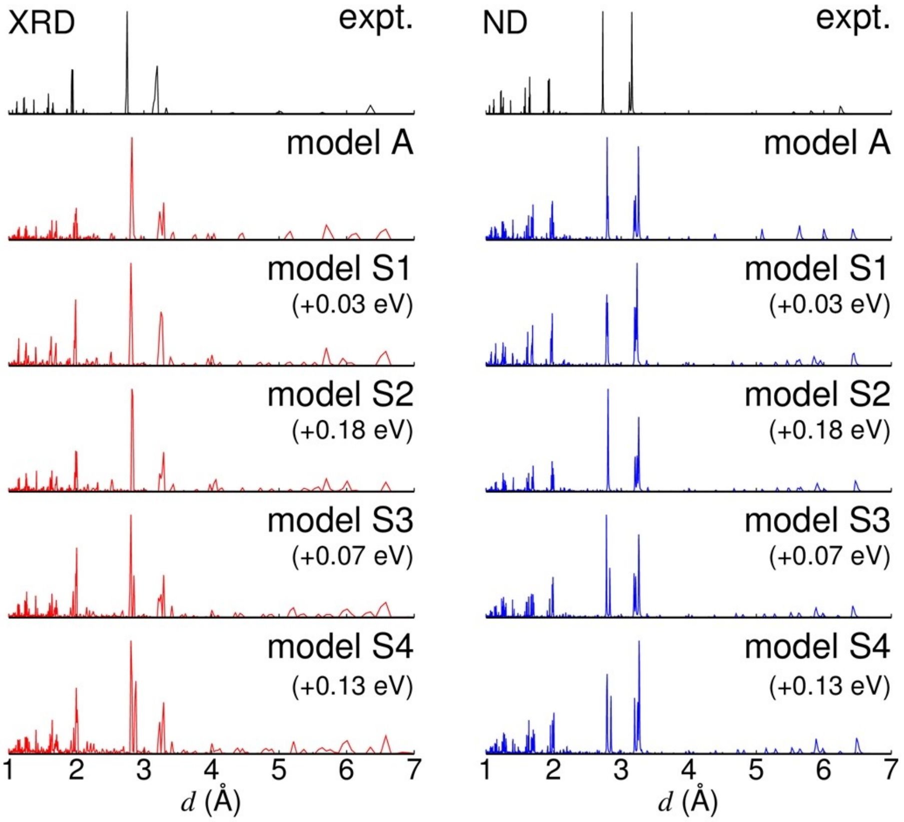

Fig. S5 Simulated synchrotron X-ray diffraction (XRD) and neutron diffraction (ND) patterns of model A and models S1–S4. Numbers in parentheses represent relative energies per the 1 × 1 × 1 unit cell with respect to model A. The experimental patterns were obtained by simulating the diffraction patterns of the structural model shown in Fig. 1a.

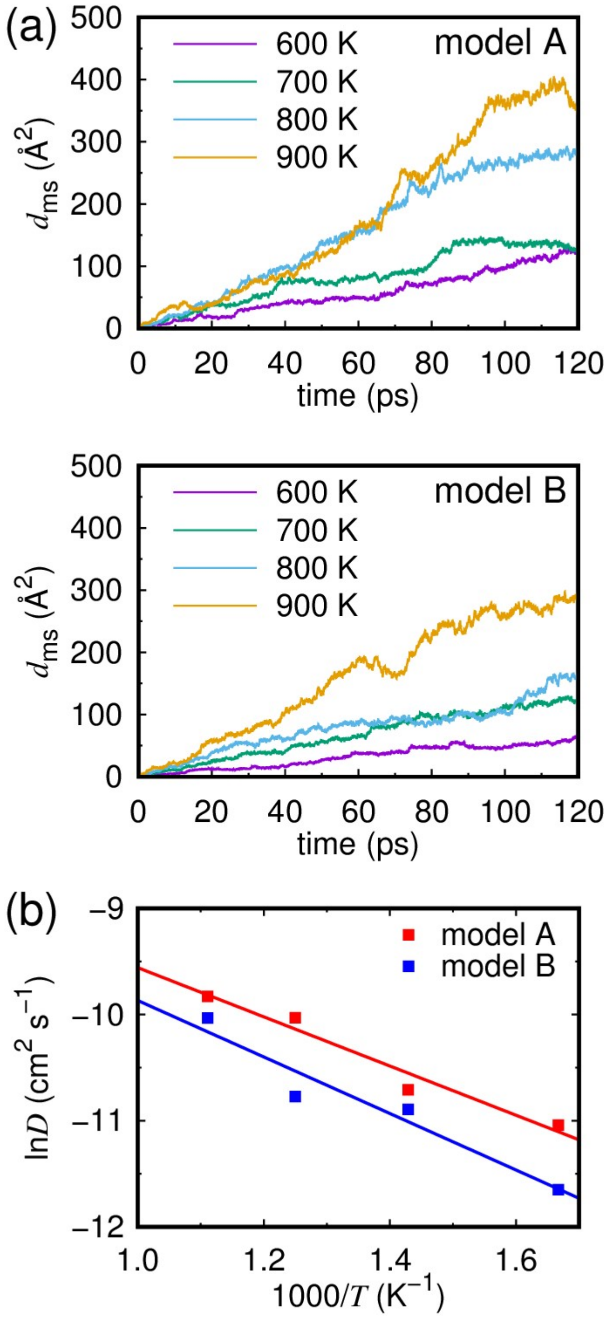

Fig. S6 (a) Mean-square displacements (d_{ms}) of Li ions as a function of time and (b) logarithmic diffusivities (ln$D$) of Li ions as a function of inverse temperature in models A and B.

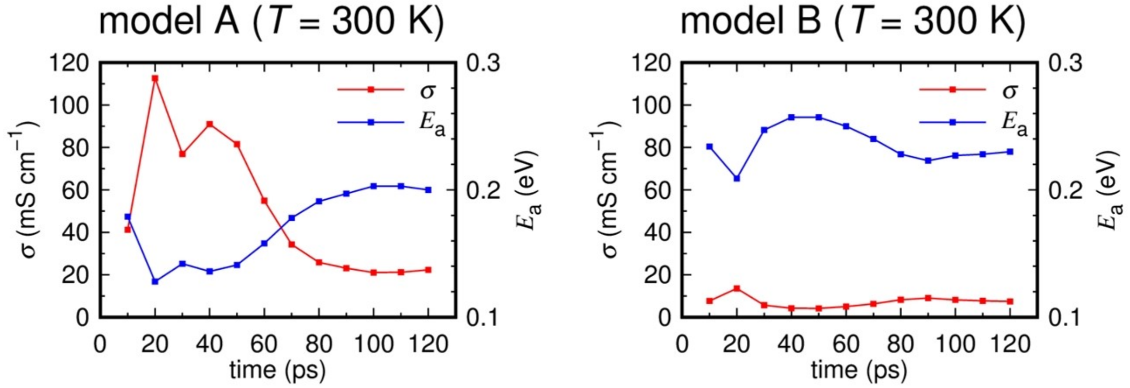

Fig. S7 Conductivity (σ) and activation energy (E_a) in LYBC as a function of time.

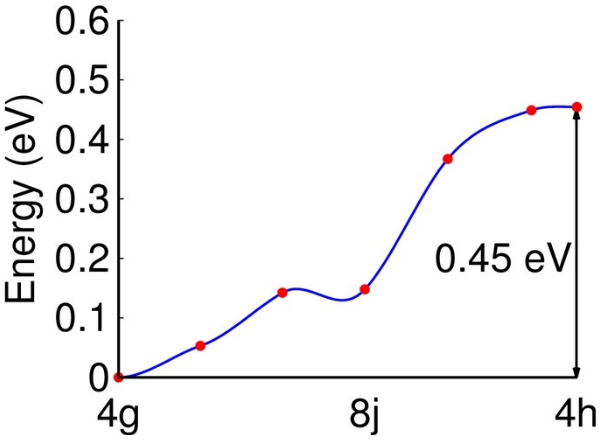

Fig. S8 Potential energy profile of a single Li ion diffusing along the vertical solid line in Fig. 3d.

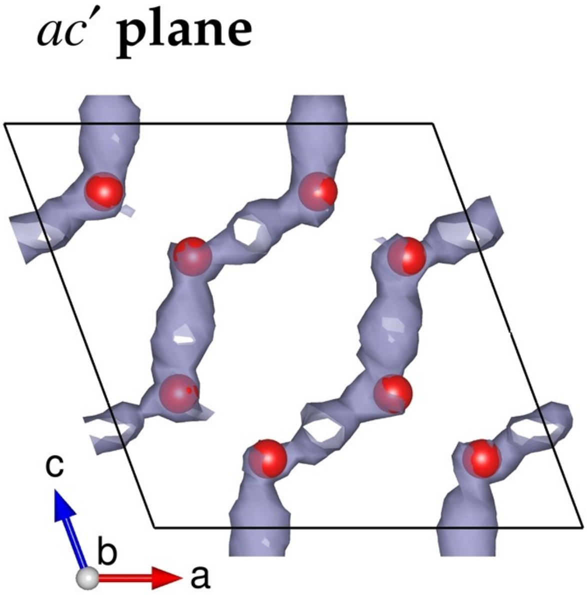

Fig. S9 Isosurfaces of the Li probability density function $P(\mathbf{r})$ of model A, obtained from the AIMD simulation at $T = 900$ K and plotted in the cross section parallel to the ac′ plane (see vertical dashed lines in Fig. 3d) with an isosurface level of 0.001 e Å^{-3}.

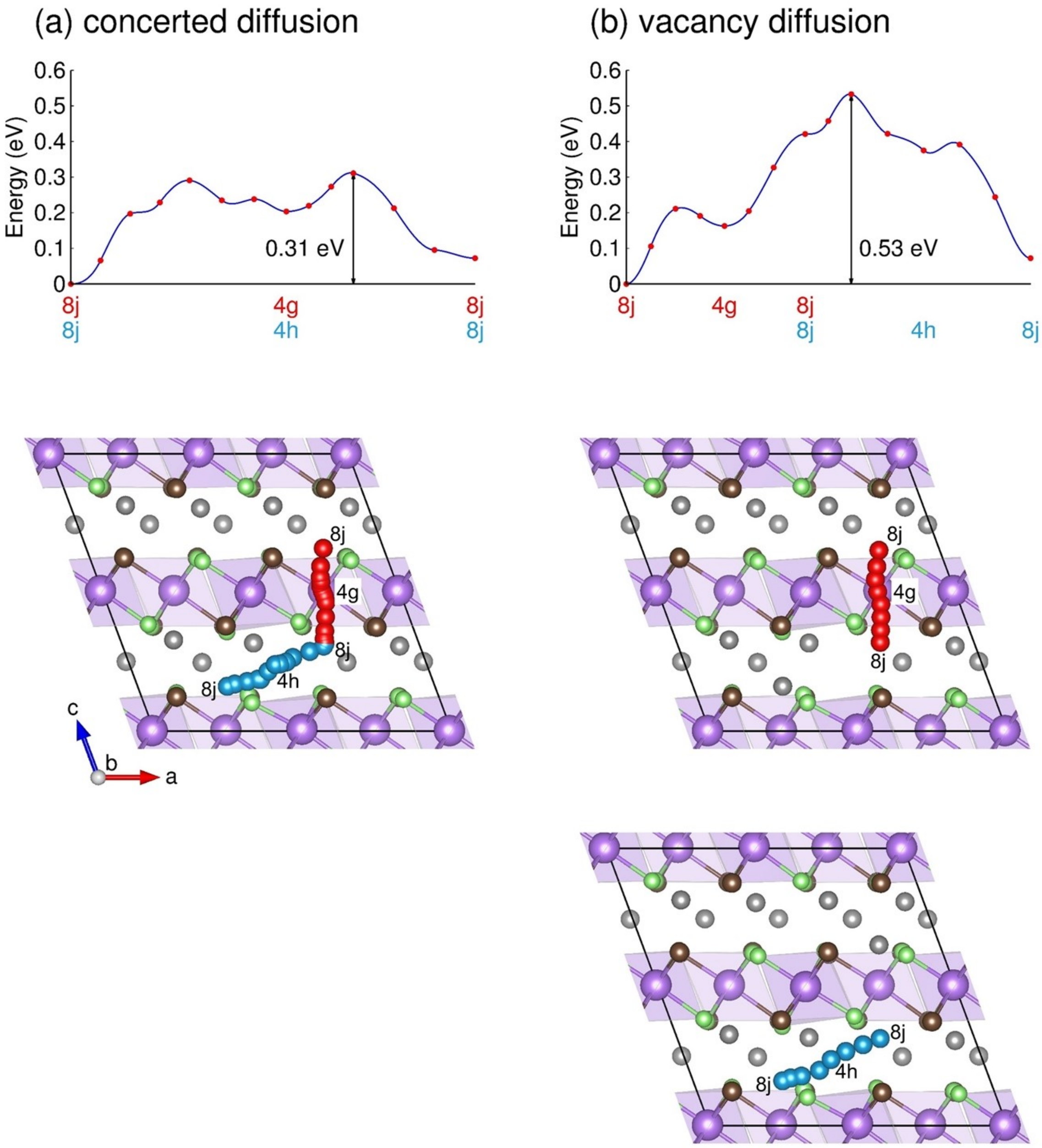

Fig. S10 Potential energy profiles and successive snapshots of Li ions diffusing along (a) concerted and (b) vacancy diffusion paths in the diagonal direction between the *a* and *c* axes in model B.

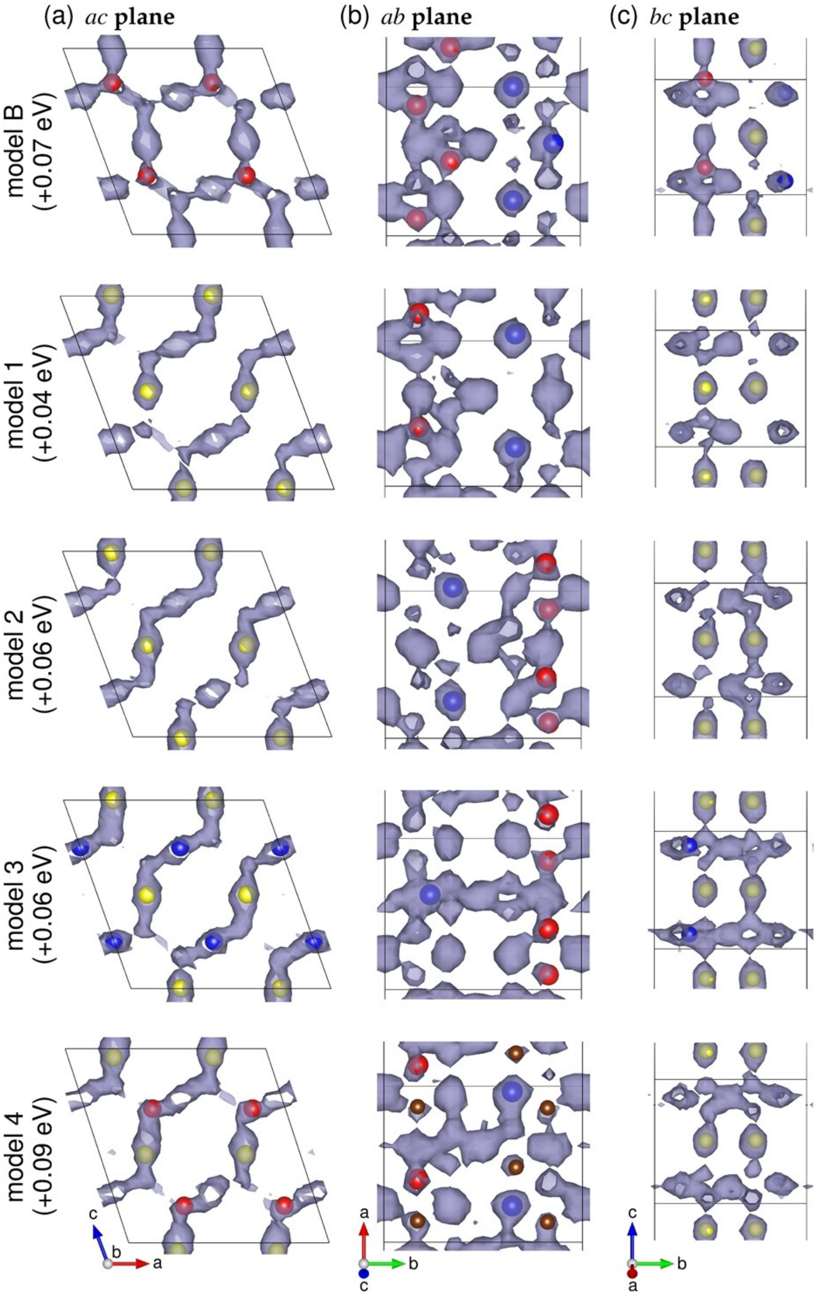

Fig. S11 Isosurfaces of the Li probability density function $P(\mathbf{r})$ of metastable LYBC structures, obtained from the AIMD simulation for 120 ps at T = 900 K and plotted in cross sections parallel to the (a) *ac*, (b) *ab*, and (c) *bc* planes with an isosurface level of 0.001 e Å^{-3}. Numbers in parentheses represent relative energies per the 1 × 1 × 1 unit cell with respect to model A. Among the atoms near the cross sections, only the Li atoms are shown. Solid lines represent the 2 × 1 × 2 unit cell.

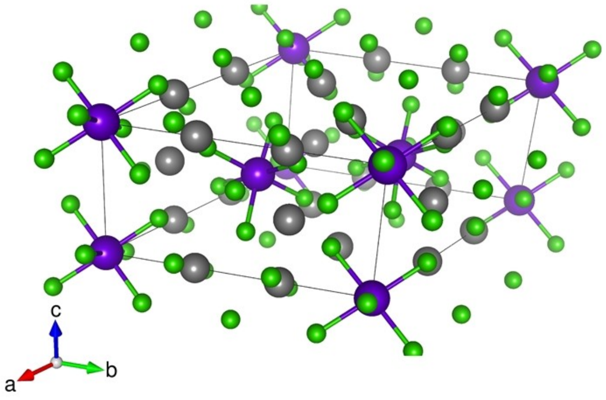
(a) LYC

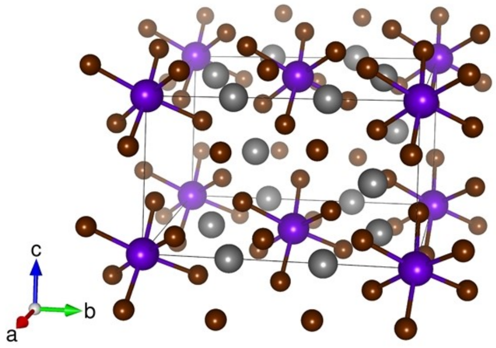
(b) LYB

Fig. S12 Ball-and-stick representation of the most stable (a) Li_3YCl_6 (LYC) and (b) Li_3YBr_6 (LYB) structures. Gray, violet, green, and brown balls represent the Li, Y, Cl, and Br atoms, respectively. Solid lines represent the 1 × 1 × 1 unit cell.

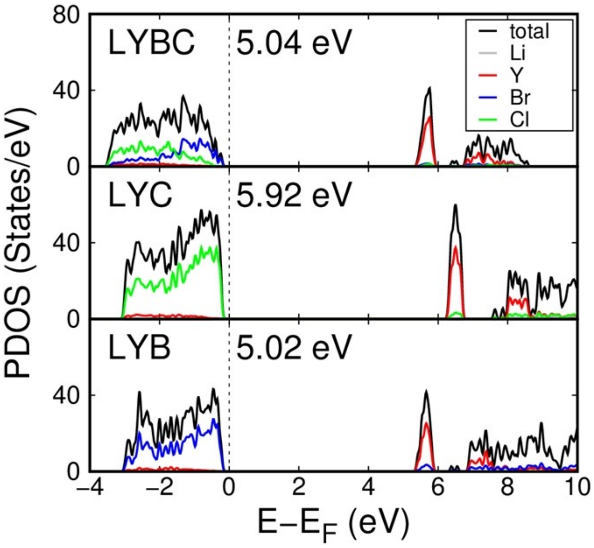

Fig. S13 Projected density of states (PDOS) of LYBC, LYC, and LYB.

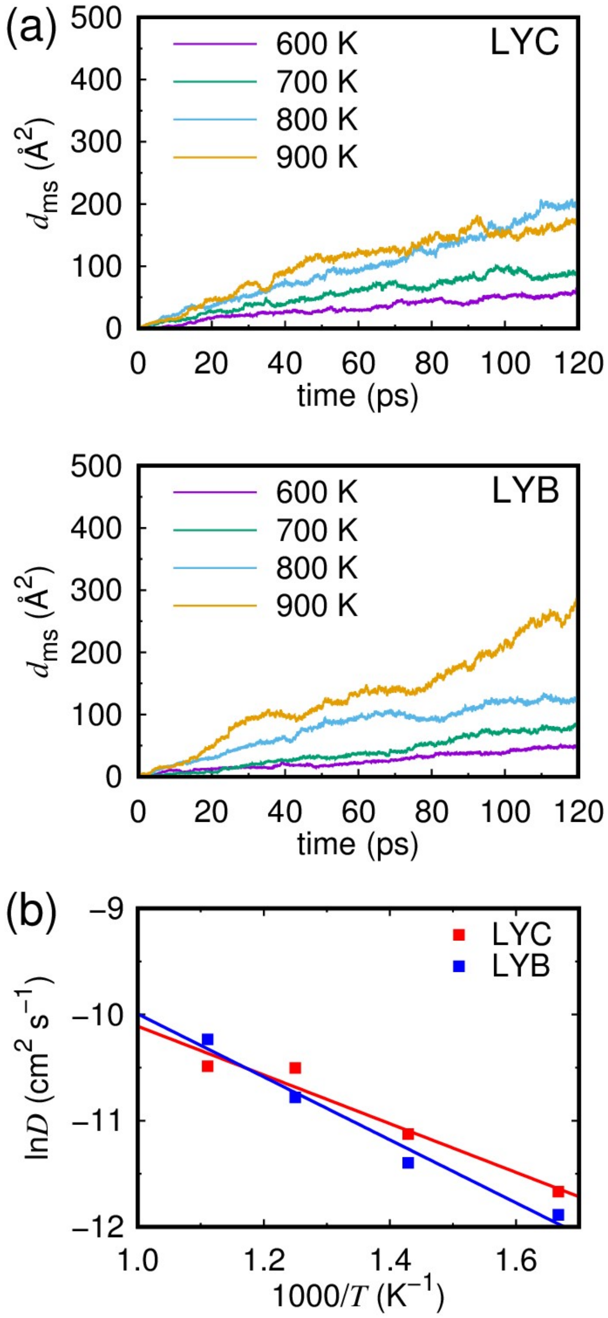

Fig. S14 (a) Mean-square displacements ($d_{\rm ms}$) of Li ions as a function of time and (b) logarithmic diffusivities (ln$D$) of Li ions as a function of inverse temperature in LYC and LYB.

(a) concerted diffusion

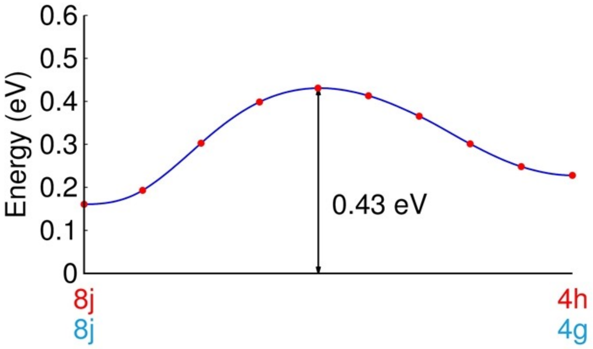

(b) vacancy diffusion

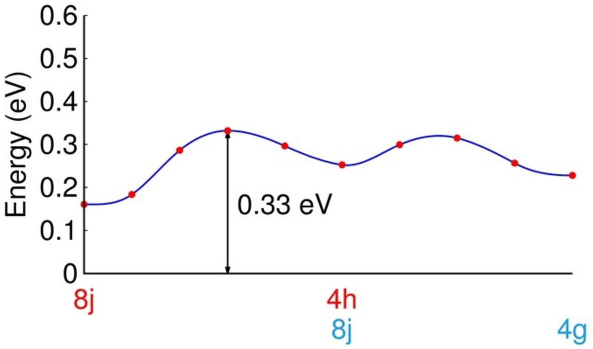

Fig. S15 Potential energy profiles of Li ions diffusing along (a) the concerted and (b) vacancy diffusion paths in LYB.

Table S1 Numbers of Li, Y, Br, and Cl atoms occupying different sites in the Y, Li, and halide layers of LYBC per the 1 × 1 × 1 unit cell. $X_A(n)$ represents n X atoms occupying the A site.

layer	this work					expt.[1]
	model A	model S1	model S2	model S3	model S4	
Y	$Y_{2a}(2)$	$Y_{2a}(1.2)$	$Y_{2a}(1.2)$	$Y_{2a}(1.2)$	$Y_{2a}(1.2)$	$Y_{2a}(1.22)$
		$Y_{4g}(0.8)$	$Y_{4g}(0.8)$	$Y_{4g}(0.8)$	$Y_{4g}(0.8)$	$Y_{4g}(0.78)$
	$Li_{4g}(3)$	$Li_{4g}(2.2)$	$Li_{4g}(2.6)$	$Li_{4g}(2.2)$	$Li_{4g}(2.6)$	$Li_{4g}(2.56)$
		$Li_{2a}(0.8)$		$Li_{2a}(0.8)$	$Li_{2a}(0.4)$	
Li			$Li_{4h}(0.8)$		$Li_{4h}(0.2)$	$Li_{4h}(1.56)$
	$Li_{2d}(1)$	$Li_{2d}(1)$	$Li_{2d}(1)$	$Li_{2d}(1)$	$Li_{2d}(0.8)$	
	$Li_{8j}(2)$	$Li_{8j}(2)$	$Li_{8j}(1.6)$	$Li_{8j}(2)$	$Li_{8j}(1.6)$	$Li_{8j}(1.88)$
					$Li_{4i}(0.4)$	
Halide	$Br_{8j}(4)$	$Br_{8j}(4)$	$Br_{8j}(4)$	$Br_{8j}(4)$	$Br_{8j}(4)$	$Br_{8j}(4.47)$
	$Br_{4i}(2)$	$Br_{4i}(2)$	$Br_{4i}(2)$	$Br_{4i}(2)$	$Br_{4i}(2)$	$Br_{4i}(1.53)$
	$Cl_{8j}(4)$	$Cl_{8j}(4)$	$Cl_{8j}(4)$	$Cl_{8j}(4)$	$Cl_{8j}(4)$	$Cl_{8j}(3.52)$
	$Cl_{4i}(2)$	$Cl_{4i}(2)$	$Cl_{4i}(2)$	$Cl_{4i}(2)$	$Cl_{4i}(2)$	$Cl_{4i}(2.48)$

Table S2 Pre-exponential factor (D_0), diffusivity (D), activation energy (E_a), and conductivity (σ) of Li ion diffusions and their errors in LYBC at $T = 300$ K.

	model A	model B
D_0 (cm^2 s^{-1})	7.2×10^{-4}	7.4×10^{-4}
error bound [D_0^{min}, D_0^{max}] (cm^2 s^{-1})	[4.5×10^{-4}, 1.2×10^{-3}]	[3.7×10^{-4}, 1.5×10^{-3}]
D (cm^2 s^{-1})	3.2×10^{-7}	1.0×10^{-7}
error bound [D_{min}, D_{max}] (cm^2 s^{-1})	[6.3×10^{-8}, 1.6×10^{-6}]	[9.6×10^{-9}, 1.1×10^{-6}]
E_a (eV)	0.20 ± 0.03	0.23 ± 0.04
σ (mS cm^{-1})	22.3	7.4
error bound [σ_{min}, σ_{max}] (mS cm^{-1})	[4.5, 111.6]	[0.7, 80.3]

References

1 Z. Liu, S. Ma, J. Liu, S. Xiong, Y. Ma and H. Chen, *ACS Energy Lett.*, 2021, **6**, 298–304.